J. Phys. B: At. Mol. Opt. Phys. 26 (1993) 2913–2925. Printed in the UK

The scattering of low energy electrons from hydrogen sulphide

R J Gulley, M J Brunger and Stephen J Buckman

Electron Physics Group, Atomic and Molecular Physics Laboratories, Research School of Physical Sciences and Engineering, Australian National University, Canberra, ACT, Australia

Received 25 March 1993, in final form 1 June 1993

Abstract. Absolute differential cross sections for vibrationally elastic electron scattering from hydrogen sulphide (H_2S) have been measured using a crossed electronic–molecular beam apparatus at incident energies from 1–30 eV and scattering angles between −20 and 130°. At each energy studied we have integrated our differential cross section data to obtain total elastic and elastic momentum transfer cross sections. Vibrational excitation of H_2S by electron impact has also been studied at incident energies of 2 and 3 eV, in the region of the low energy shape resonance. Both our differential and integral cross sections are compared with previous experimental studies and calculated values.

1. Introduction

The study of electron scattering from the hydrogen sulphide (H_2S) molecule is of both practical and fundamental interest. As it has a relatively large dipole moment (0.98 Debye), one may expect the low energy electron scattering cross sections to be large, a feature which has been demonstrated in many polar molecules. Indeed, the presence of such polar molecules in a gas, even as a minor impurity, can have a significant effect on the physical properties of the gas, such as the electrical conductivity. In addition H_2S is known to be a common constituent of interstellar molecular clouds so there is also interest due to its astrophysical applications.

From a fundamental point of view the H_2S molecule represents one of the simpler non-linear, closed shell, polar polyatomic molecules and consequently has been the subject of several theoretical electron scattering calculations. The first quantum calculations were carried out by Gianturco and Thompson (1980), using a parametrized model to treat exchange and polarization forces. This was followed by the parameter-free model calculations by Jain and Thompson (1983), Gianturco (1991), and the complex-Kohn variational calculations of Lengsfield *et al* (1992). The cross sections determined by these calculations were computed within the framework of the fixed-nuclei approximation (FNA), which has led to convergence problems when applied to polar polyatomic molecules (see the review by Norcross and Collins (1982)). These problems were circumvented via a modification of the spatial partitioning of the scattering system, first suggested by Rescigno *et al* (1982), in which a description of higher order partial wave ($l > 6$) contributions are given by the Born approximation, whilst a description of $l \leqslant 6$ contributions are given either by the usual close-coupling (Jain and Thompson 1983, Gianturco 1991) or Kohn (Lengsfield *et al* 1992) approaches. Lengsfield *et al* have also included polarization and correlation effects via the use of an *ab initio* optical potential, and their previous calculations for electron–NH_3 scattering (Lengsfield *et al* 1992) agreed favourably with measurements taken in this laboratory (Alle *et al* 1992). The calculations of both Jain and Thompson and

0953-4075/93/172913+13$07.50

Gianturco also addressed the classification of the low energy shape resonances observed in electron scattering and dissociative attachment experiments on H_2S.

Previous experimental investigations of scattering of electronics from H_2S have been limited. Absolute total cross sections have been reported by Sokolov and Sokolova (1981) who based their experiment on an electron cyclotron resonance technique, and by Szmytkowski and Maciag (1986) who employed a linear transmission experiment. Angular distributions for elastic electron–H_2S scattering in the energy range 10–80 eV were measured by Marinkovic (1985). However these data are not absolute and quantitative conclusions, other than the angular variation of the cross section, cannot be deduced from them. The only absolute differential cross sections currently available in the literature, for the energy regime of the present study, are the measurements of Rohr (1978) for both elastic scattering and for the excitation of the stretching (100 + 001) and bending (010) modes for collision energies up to 10 eV. The vibrational excitation measurements revealed, for the first time, the presence of a strong threshold resonance for the symmetric + asymmetric stretching modes (325 meV) and also a broad shape resonance at 2.3 eV, which had previously been observed in dissociative attachment (Fiquet-Fayard *et al* 1972) and electron transmission (Sanche and Schulz 1973) experiments. The measurements of Rohr were placed on an absolute scale by comparing the elastic scattering rates in H_2S with those for helium and using the elastic helium cross sections of Andrick and Bitsch (1975) as the normalization standard. The resulting absolute scale for these measurements was estimated to have a large uncertainty (a factor of two). Thus the main motivation for the present work was to provide accurate, absolute experimental cross sections for comparison with the recent theoretical work.

In the next section we discuss details of the experimental procedure employed in the current measurements, including the method of normalization. A discussion of our results are presented in section 3, with conclusions being drawn in section 4.

2. Experimental apparatus and procedures

The experimental apparatus employed in the present measurements is described elsewhere in detail by Brunger *et al* (1990, 1991) and so only a brief description will be given here.

A beam of H_2S effusing from a multichannel capillary array, with an active diameter of 1 mm, was crossed with an incident beam of monoenergetic electrons produced by a conventional thermionic source. Both the incident and scattered electrons were transported and energy analysed by a combination of electrostatic electron optics and a hemispherical analyser. The scattered electron analyser was rotated about the molecular beam providing access to scattering angles between $-20°$ and 130°. The true 0° position was determined (to within $\pm 1°$) as that about which the intensity of elastically scattered electrons was symmetric.

The incident electron energy was calibrated against the $1s2s^2\ ^2S$ resonance in helium at 19.367 eV (Brunt *et al* 1977). The overall energy resolution of the spectrometer was typically 65 meV (FWHM), which was sufficient to resolve the vibrationally elastic scattering from the (010) bending mode (0.147 meV energy loss) and composite (100, 001) stretching modes (0.324, 0.326 meV energy loss) excitations. A typical energy loss spectrum is shown in figure 1.

The absolute scale of the H_2S elastic cross section, at a given energy and scattering angle (θ), was determined by the use of the relative flow technique (Nickel *et al* 1989),

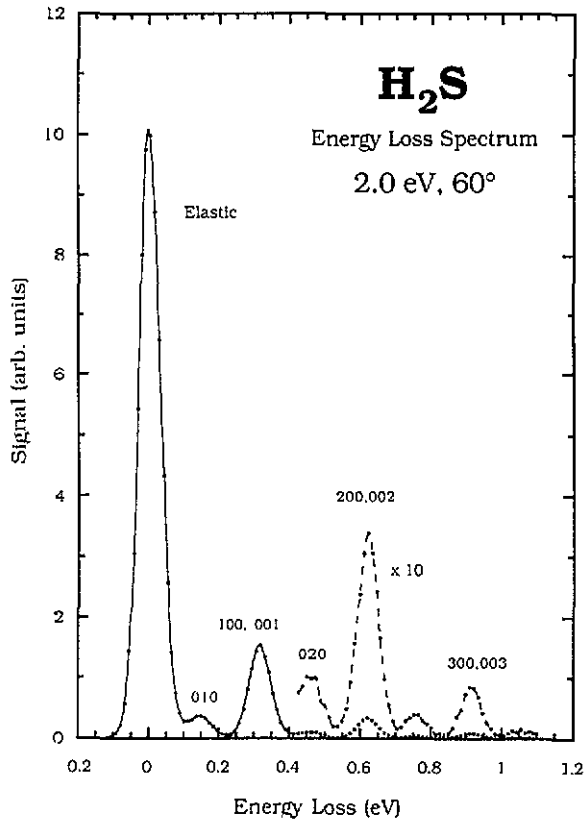

Figure 1. Electron energy loss spectrum for H_2S at an incident energy of 2.0 eV. and a scattering angle of 60°.

using helium as a 'standard' cross section. This technique relates the elastic differential cross section for H_2S to that for helium via the relation

$$\frac{d\sigma}{d\Omega}(\theta)_{H_2S} = \frac{I_{He}}{I_{H_2S}} \frac{N_e(\theta)_{H_2S}}{N_e(\theta)_{He}} \frac{(Fm^{0.5})_{He}}{(Fm^{0.5})_{H_2S}} \frac{d\sigma}{d\Omega}(\theta)_{He} \tag{1}$$

where I is the electron beam current, $N_e(\theta)$ the scattered electron count rate, F the flow rate through the capillary array and m the molecular weight. The final term in (1), $d\sigma/d\Omega(\theta)_{He}$, is the 'known' elastic differential cross section for helium. Below the onset of the $n = 2$ inelastic threshold of helium ($\approx$ 19.8 eV), we have used *ab initio* variation calculations of Nesbet (1978) for this cross section. For energies above this threshold, the values used were the experimental results of Brunger *et al* (1992).

The relative flow rates, as a function of driving pressure, were determined from a separate series of measurements. As in the case of our previous measurements for NH_3, a plot of the normalized flow rates ($Fm^{0.5}$) plotted against driving pressure for both H_2S and He revealed two curves that can differ by as much as 10%. Although such differences are likely to be apparatus specific, it is important to note that they do occur and it is thus imperative that the flow rates are actually measured in such experiments. From these data, the ratio $(Fm^{0.5})_{He}/(Fm^{0.5})_{H_2S}$ was determined as a function of the ratio of the driving pressures behind the capillary P_{He}/P_{H_2S} for the pressure range of interest. This procedure

has been discussed previously (Alle *et al* 1992). During the scattering experiments, the capillary driving pressure for both gases was chosen such that their mean free paths in the region at the entrance to the capillary array were the same. Under this condition, it is assumed that the scattering volume was identical for each gas as long as intermolecular collisions did not have a significant effect on the shape of the gas beam profile. Recent measurements of the spatial profiles of effusive molecular beams formed by a capillary array support this assumption (Buckman *et al* 1993). This work has shown that the effects of intermolecular or wall collisions are negligible as long as the mean free path of the gas is greater than approximately twice the capillary diameter.

We have adopted a slightly different method of applying the relative flow normalization technique than in our previous work (e.g. Alle *et al* 1992). In these previous studies we followed a procedure in which (i) the scattering geometry at each energy and angle was checked by comparing the *shape* of our relative angular distributions for elastic e^-–He scattering with those calculated by Nesbet (1979), (ii) the angular distributions for the target gas were then measured and (iii) these distributions were subsequently placed on an absolute scale by relative (to helium) flow measurements at a few selected scattering angles. Background contributions at each scattering angle were determined by measurements of the scattered electron intensities when the gas entered the vacuum chamber, at an equivalent flow rate, through a second capillary located at the periphery of the scattering chamber.

However, for the present study we have performed the relative flow normalization independently at each scattering angle. This involves the measurement of the ratio of scattering intensities, electron beam currents and driving pressures for both helium and hydrogen sulphide at each scattering angle. We have also changed our gas handling facility such that both gases are present in the scattering chamber at all times. For the measurements of the scattered electron count rates either H_2S was directed to the capillary array and helium to the background capillary or vice-versa. Background contributions were measured by routing both gases through the background capillary and measuring the associated electron count rates. The main advantages of these changes to the procedure are (i) shifts in contact potential, which can occur by alternating between gases, are avoided by having both gases present in the vacuum chamber, (ii) each measurement of an intensity ratio at a particular angle takes approximately 30 min, thus minimizing the effects of drifts in potentials applied to the electron optical elements, electron beam current and target beam density and (iii) the measured cross sections are less sensitive to the size of the target region (the electron beam/molecular beam overlap). One disadvantage of this technique, which has been used successfully by Shi and Burrow (1992), is that the background contribution is slightly larger with both gases entering the chamber at the same time.

The cross sections for vibrationally inelastic scattering were placed on an absolute scale by measuring the ratio of the various inelastic scattering intensities at each angle to that for elastic scattering. The procedure employed for these measurements is described elsewhere (Gulley *et al* 1992). We again note the importance of ensuring that the transmission efficiency of the scattered electron analyser is optimized over the required energy loss range for such measurements. In our case this requires ramping the mid-element potential of our three element analyser zoom lens synchronously with that of the energy loss potential, to maintain a constant focal length and magnification of the zoom lens.

The measured elastic differential cross sections were extrapolated to both 0° and 180° using the *shape* of the theoretical cross sections of Lengsfield *et al* (1992) as a guide. The only exception to this was at 10 eV where the calculation of Gianturco (1991) was employed, as values from the Kohn theory are not available at this energy. These data were then integrated to give the experimental total elastic and momentum transfer cross sections.

The measurement of the cross section ratios at each angle were performed many times under a variety of different experimental conditions. Rather than use the raw statistical uncertainties in calculating the final statistical contribution to the absolute error, we have used the standard deviation of the complete set of ratio measurements at each angle. In almost all circumstances this figure is larger than the raw statistical value, which was less than 1%, but we believe it may provide a better indication of the real uncertainty involved in the measurement. The total absolute uncertainty then results from the addition of the statistical uncertainty and the uncertainty in the measurement of the various experimental parameters. This measurement uncertainty is obtained from the addition, in quadrature, of uncertainties in the relative flow rates calibration (4%), gas pressure (2%), beam current ratios (4%) and an uncertainty in the 'known' helium cross sections (2% below 20 eV, 4% above).

3. Results and discussion

3.1. Elastic scattering

Absolute differential cross sections for elastic electron scattering by H_2S are given in table 1. The figures in brackets, indicating the absolute uncertainty in these cross sections, vary between about ±6.5% and ±11.5%, typical values being in the region of ±7-8%. Representative examples of the cross section data 1.0, 2.0, 3.0, 5.0, 15 and 30 eV can be found in figures 2–7 respectively.

In figure 2, the DCS at 1.0 eV is compared with the Kohn variational calculation of Lengsfield *et al* (1992) and the model calculations of Jain and Thompson (1983) and Gianturco (1991). The latter calculation clearly overestimates the cross section at all but the most forward of scattering angles. Both the Kohn calculation and the model calculation of Jain and Thompson show a good representation of the experimental cross section in both the overall shape and absolute magnitude. Neither calculation appears to predict the weak structure which is evident at intermediate scattering angles (60–90°) in the experimental cross section. At an energy of 2 eV (figure 3) this structure has developed into a minimum in the DCS at 60° and the magnitude of the elastic cross section for angles larger than about 30° has increased by a factor of two. This change is also reflected in the Kohn calculation which accurately reproduces the shape of the experimental cross section but is uniformly higher over the entire angular range. The calculation of Gianturco is closer in magnitude to the measured cross section at this energy but does not show any evidence of the first minimum, rather showing a single minimum at around 90°.

At 3 eV (figure 4), we make a comparison with the only other absolute cross section available in the literature, that of Rohr (1978). Whilst there is some similarity in shape between the two measurements, the absolute values differ by over a factor of two at some angles. Rohr placed a rather conservative estimate of a factor of two on his absolute values and it appears that this may be appropriate. Once again there is a reasonable level of agreement with the calculations of Jain and Thompson and Lengsfield *et al*, particularly at scattering angles less than about 60°. At larger angles there is perhaps better agreement with the values of Jain and Thompson, although both calculations predict the overall features observed by experiment, the main difference being in the relative strength of the cross section minima. At 5 eV (figure 5), there is again good agreement with the Kohn calculation, particularly at backward scattering angles. Somewhat surprisingly, the theory is substantially lower than the experimental values at scattering angles between 15 and 80°.

Table 1. Elastic differential cross sections for H_2S in $Å^2\ sr^{-1}$ and integral cross sections in $Å^2$. The figures in brackets represent the absolute uncertainty.

	Energy (eV)							
Angle	1.0	2.0	3.0	5.0	10.0	15.0	20.0	30.0
10					18.32 (1.75)			23.11 (1.71)
15	13.87 (1.6)	7.89 (0.72)	7.41 (0.79)	9.91 (0.83)		16.03 (1.56)	15.53 (1.19)	
20	7.53 (0.61)	5.35 (0.38)	5.64 (0.42)	8.30 (0.53)	11.42 (0.74)	12.86 (0.93)	11.38 (0.91)	10.26 (0.76)
25						10.01 (0.65)	8.42 (0.70)	
30	3.65 (0.26)	2.84 (0.19)	3.41 (0.22)	5.40 (0.35)	7.45 (0.50)	7.54 (0.59)	5.98 (0.53)	4.18 (0.33)
40	1.95 (0.14)	1.73 (0.11)	2.30 (0.18)	3.70 (0.24)	4.35 (0.28)	4.03 (0.33)	2.97 (0.22)	1.53 (0.12)
50	1.21 (0.08)	1.31 (0.09)	1.65 (0.12)	2.56 (0.16)	2.19 (0.15)	1.87 (0.21)	1.15 (0.09)	0.456 (0.034)
55								0.246 (0.020)
60	0.867 (0.061)	1.22 (0.08)	1.37 (0.09)	1.84 (0.12)	1.01 (0.07)	0.749 (0.079)	0.367 (0.028)	0.136 (0.010)
65				1.67 (0.11)		0.490 (0.041)	0.240 (0.025)	0.122 (0.010)
70	0.796 (0.052)	1.33 (0.010)	1.35 (0.11)	1.55 (0.10)	0.595 (0.038)	0.349 (0.028)	0.209 (0.023)	0.144 (0.010)
75				1.45 (0.09)		0.333 (0.023)	0.242 (0.019)	0.200 (0.015)
80	0.750 (0.049)	1.41 (0.09)	1.28 (0.09)	1.36 (0.09)	0.569 (0.044)	0.392 (0.043)	0.304 (0.026)	0.257 (0.019)
90	0.643 (0.050)	1.38 (0.09)	1.20 (0.08)	1.22 (0.08)	0.648 (0.042)	0.518 (0.037)	0.418 (0.030)	0.336 (0.024)
100	0.529 (0.038)	1.22 (0.08)	1.07 (0.07)	1.01 (0.07)	0.622 (0.051)	0.578 (0.050)	0.455 (0.034)	0.350 (0.026)
110	0.431 (0.035)	1.035 (0.07)	0.950 (0.069)	0.871 (0.060)	0.582 (0.041)	0.541 (0.049)	0.382 (0.029)	0.303 (0.024)
115				0.820 (0.054)				
120	0.370 (0.024)	0.962 (0.068)	0.926 (0.062)	0.843 (0.054)	0.530 (0.034)	0.422 (0.030)	0.270 (0.022)	0.208 (0.019)
130	0.430 (0.041)	1.078 (0.070)	1.09 (0.07)	1.16 (0.075)	0.664 (0.048)	0.329 (0.023)	0.168 (0.015)	0.103 (0.009)
Q_T	26.3 (5.3)	26.0 (5.2)	25.1 (5.0)	31.1 (6.2)	26.2 (5.2)	22.9 (4.6)	18.0 (3.6)	14.8 (3.0)
Q_M	8.1 (1.6)	18.9 (3.8)	17.0 (3.4)	21.8 (4.4)	12.8 (2.6)	8.3 (1.7)	5.2 (1.0)	3.3 (0.66)

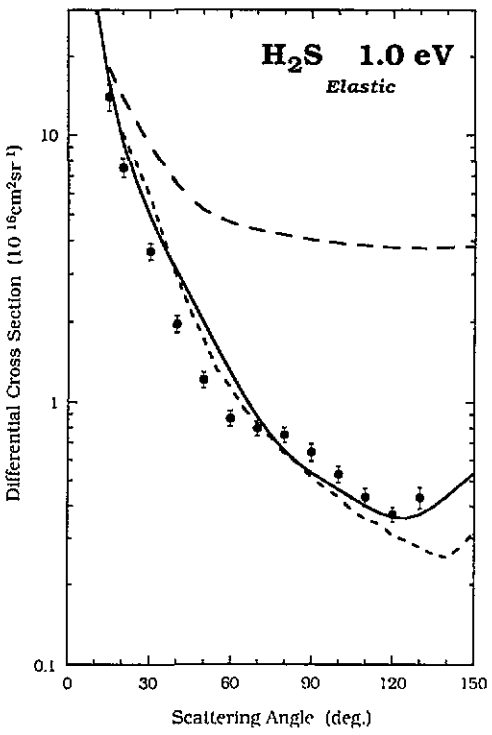

Figure 2. Differential cross section for elastic electron scattering from H_2S at 1.0 eV. Present data, ●; Gianturco, — — —; Jain and Thompson, - - -; Lengsfield *et al*, ——.

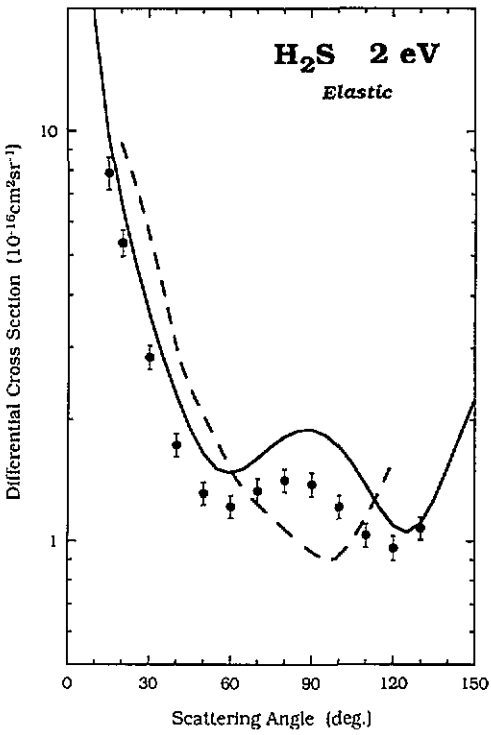

Figure 3. Differential cross section for elastic electron scattering from H_2S at 2.0 eV. Present data, ●; Gianturco, — — —; Lengsfield *et al*, ——.

At both 15 and 30 eV (figures 6 and 7) we can compare the present results with the relative differential cross sections of Marinkovic (1985) by normalizing the latter to our result at a scattering angle of 100°. The level of agreement is excellent. The only significant differences occur in the region of the cross section minimum where the deeper minima obtained with the present apparatus is probably due to higher angular resolution. Similar behaviour is also observed at both 10 and 20 eV (not shown). At 15 eV, the Kohn variational calculation once again shows good agreement with the experimental cross section, particularly at forward angles. This is not the case however at 30 eV where the level of agreement with experiment is perhaps the worst for any of the energies studies. Although the theoretical cross section has the same general shape as that of the experiment it appears to overestimate the cross section at all but the most forward angles (< 20°). On the other hand the calculation of Gianturco is in good agreement with the present cross section across the entire angular range.

The integral cross sections, total elastic and elastic momentum transfer, which have been derived from the DCS measurements, are shown in figures 8 and 9 respectively where they are also compared with total elastic cross sections from the various theories and with the grand total cross section of Szmytkowski and Maciag (1986). The uncertainties in the present integral cross sections are estimated to be ±20%. The total elastic cross section is, as expected, less than the grand total cross section, particularly above 2 eV where the influences of inelastic events other than vibrational and rotational excitation (dissociative attachment, electronic excitation and ionization) are evident. Both integral cross sections,

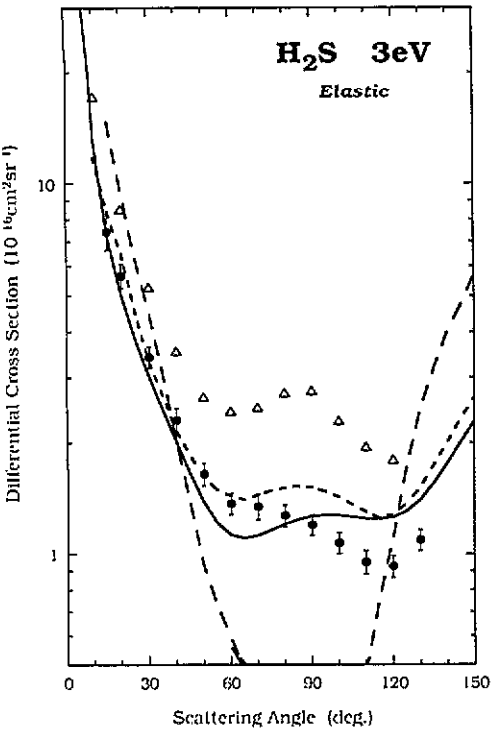

Figure 4. Differential cross section for elastic electron scattering from H_2S at 3.0 eV. Present data, ●; Rohr, △; Gianturco, — — —; Jain and Thompson, – – –; Lengsfield *et al*, ——.

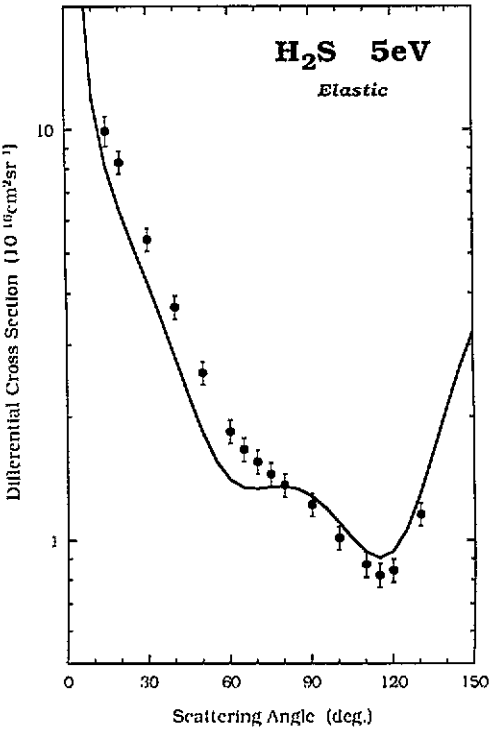

Figure 5. Differential cross section for elastic electron scattering from H_2S at 5.0 eV. Present data, ●; Lengsfield *et al*, ——.

but in particular the momentum transfer, exhibit a deep Ramsauer-like minimum at around 1–2 eV. This is unlikely to be due to the same physical processes that lead to the Ramsauer–Townsend minima in many spherical symmetric atomic and molecular systems but rather to a transition between a steeply decreasing cross section at low energies which results from the dominance of the dipole interaction, to a region where other interactions and the onset of inelastic processes, some of which are resonantly enhanced above 2 eV, begin to dominate the cross section. There is a large amount of experimental evidence (see, for example, Sanche and Schulz 1973, Azria *et al* 1979, Rohr 1978 and references therein) for the existence of transient negative ions of H_2S and its disassociative fragments, in the energy region below 10 eV. In figure 8, structure is evident in both the total elastic and grand total cross sections though they appear to be more dominant, as expected, in the latter. The presence of such structure in the total elastic cross section indicates that some of the transient resonances must decay via this channel. At energies below about 5 eV, the present data is in good accord with the total elastic cross section of Jain and Thompson, whilst above 10 eV the agreement with both Gianturco and Lengsfield *et al* is also good.

3.2. Vibrational excitation

Differential cross sections for the excitation of the first bending mode (010) and the composite symmetric + asymmetric stretch (100 + 001) have been measured at both 2.0 and 3.0 eV and tabulated values are given in table 2. The estimated absolute uncertainty in the cross sections lie between 15 and 17%. Both of these energies lie within the range of

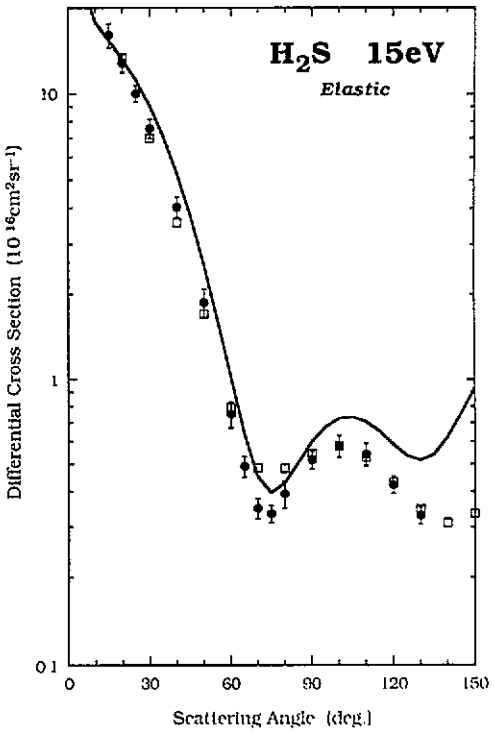

Figure 6. Differential cross section for elastic electron scattering from H_2S at 15 eV. Present data, ●; Marinkovic, □; Lengsfield *et al*, ——.

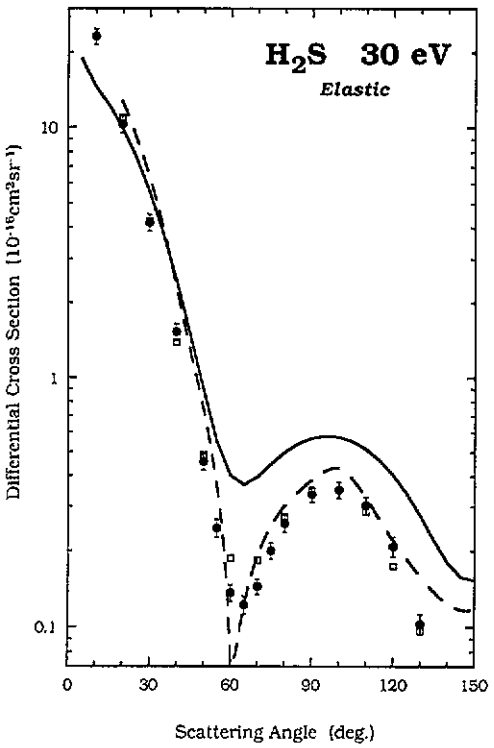

Figure 7. Differential cross section for elastic electron scattering from H_2S at 30 eV. Present data, ●; Marinkovic, □; Lengsfield *et al*, ——.

influence of the broad shape resonance centred at around 2.3 eV (Rohr 1978). Examples of these cross sections at 2.0 eV are shown in figures 10(*a*) and (*b*) and at 3.0 eV in figure 11. At 2.0 eV we can compare directly with the experimental results of Rohr and the calculation of Jain and Thompson (1983), although in the case of the stretch modes their calculation is for the (100) symmetric stretch only. In figure 10(*a*), the theoretical cross section has been scaled down by a factor of three whilst in figure 10(*b*), the experimental results of Rohr have been scaled down by a factor of two. Thus when one compares these results the picture which arises is a little confusing. On the one hand for the bending vibration (figure 10(a)), we are in fair agreement in absolute terms with the measurements of Rohr, but both are a factor of two lower than the theory. On the other hand for the composite (100 + 001) excitation, the present measurements are a factor of two lower than Rohr's but in good agreement in both shape and magnitude with the theory (for the (100) mode only). The experimental discrepancy between the present data and that of Rohr can only be explained by a substantial difference in the transmission of the energy analysers used in the two experiments.

There has also been some uncertainty as to the nature of the low lying structures observed in both vibrational excitation and dissociative attachment cross sections. Fiquet-Fayard *et al* (1972) observed the 2.3 eV resonance in dissociative attachment experiments and assigned it as a state of $^2A_1$ symmetry which arose from the addition of an electron to the lowest unoccupied molecular orbital ($6a_1$) of H_2S^-. Rohr concurred with this assignment, based on the interpretation that his measured angular distributions for vibrational excitation were isotropic and thus consistent with the dominant s-wave scattering that the above assignment

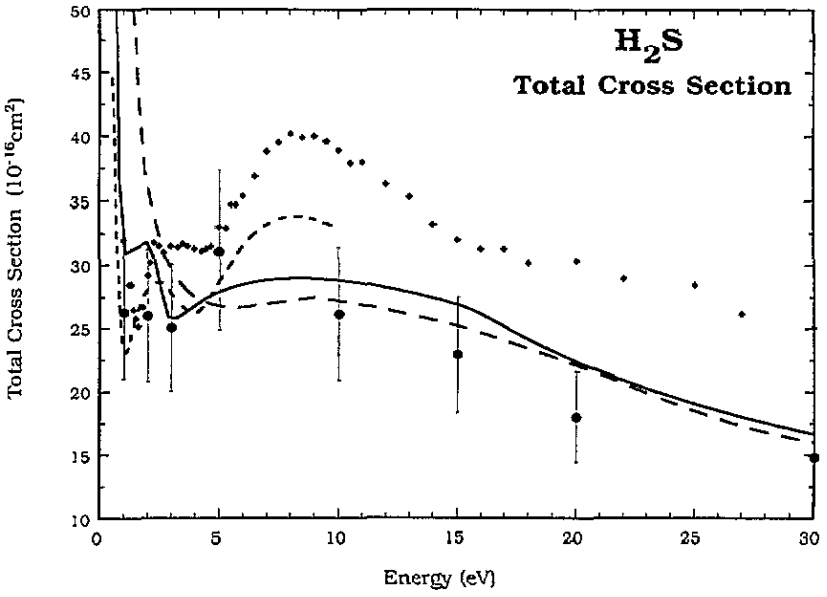

Figure 8. Total cross sections for elastic electron scattering by H_2S. Total elastic cross section: present results, ●; Jain and Thompson, – – –; Gianturco, — — —; Lengsfield *et al*, ——. Grand total cross section: Szmytkowski and Maciag, ♦.

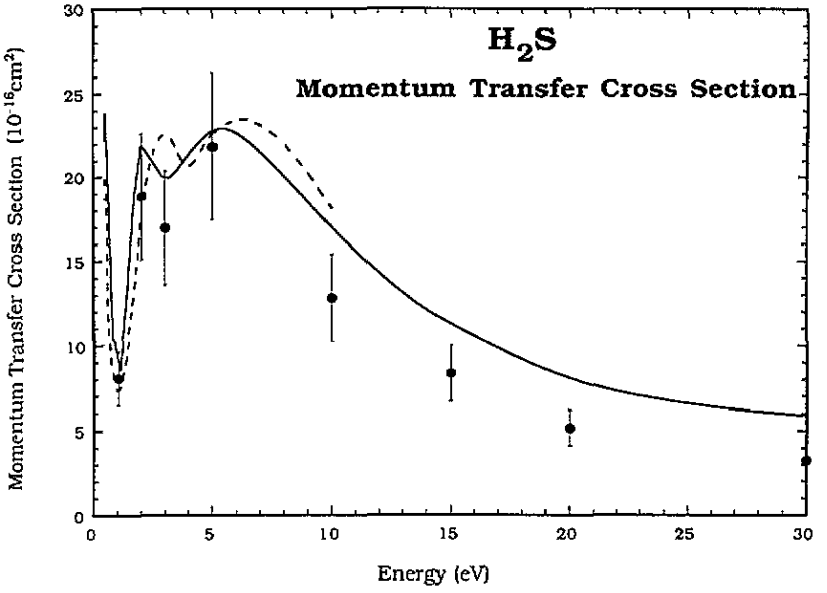

Figure 9. The momentum transfer cross section for elastic electron scattering by H_2S. Present cross section, ●; Jain and Thompson, – – –; Lengsfield *et al*, ——.

demands. However, such a shape resonance cannot occur in the s-wave due to the lack of

Table 2. Differential cross sections (in $Å^2$ sr^{-1}) for the excitation of the 010 and 100+001 vibrational modes of H_2S. The estimated uncertainty in each value is ±15%.

	Energy (eV)			
	2.0		3.0	
Angle	010	100+001	010	100+001
20	0.076	0.260	0.068	0.165
30	0.062	0.222	0.058	0.147
40	0.053	0.194	0.049	0.126
50	0.050	0.194	0 047	0.110
60	0.049	0.190	0.050	0.102
70	0.052	0.209	0.054	0.107
80	0.058	0.225	0.062	0.109
90	0.060	0.232	0.064	0.113
100	0.059	0.227	0.064	0.115
110	0.058	0.212	0.060	0.115
120	0.063	0.208	0.053	0.117
130	0.059	0.186	0.049	0.112

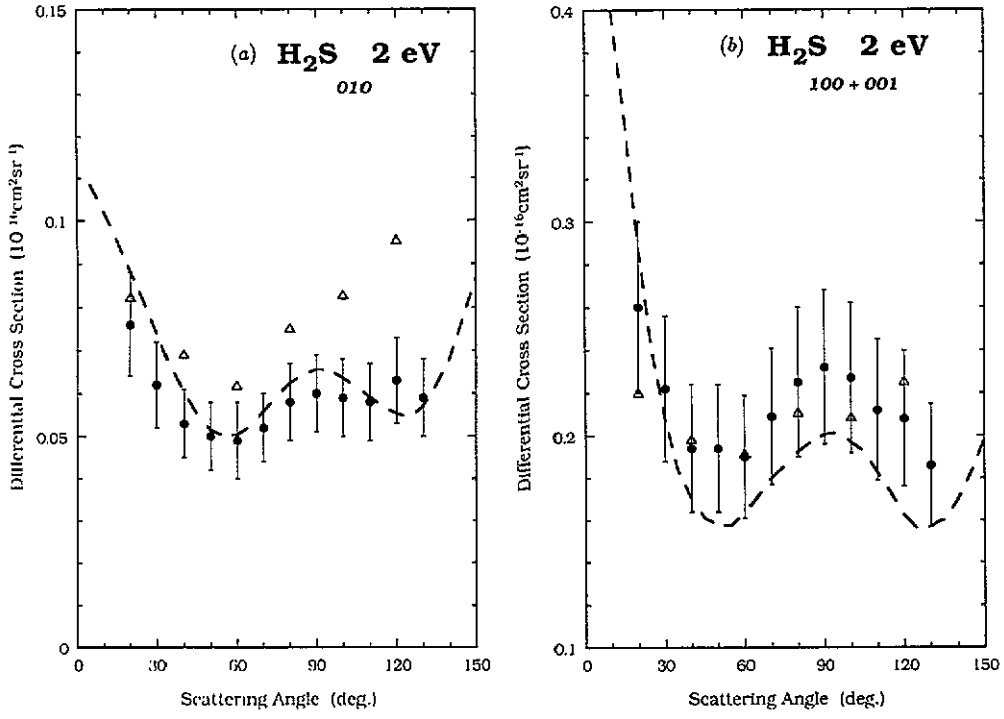

Figure 10. Differential cross section at 2.0 eV for (*a*) the excitation of the first bending mode (010) of H_2S: present data. ●; Rohr, △; Jain and Thompson, – – – scaled by a factor of 0.33 and (*b*) the excitation of the 100 + 001 stretching modes: present data, ●; Rohr, △ (scaled by a factor of 0.5); Jain and Thompson, – – –.

an angular momentum barrier and, as a result, if the observed feature was to be associated with the $^2A_1$ symmetry, it must occur in a higher angular momentum partial wave. A

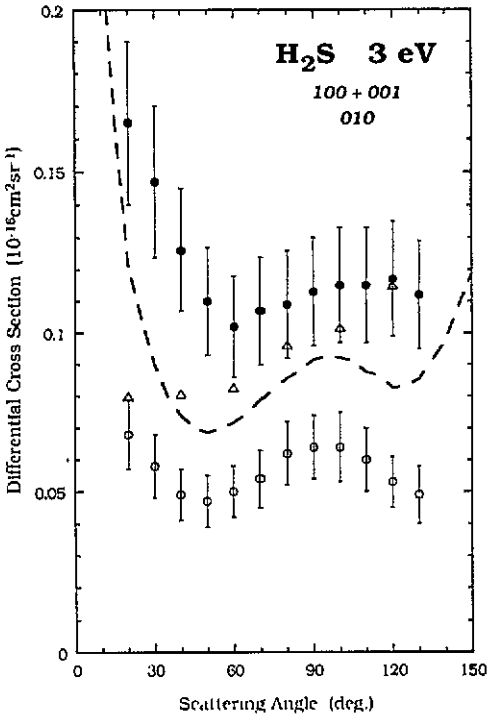

Figure 11. Differential cross sections for the excitation of the 010 and 100 + 001 vibrational bands at 3.0 eV. For the 100 + 001 excitation: present data, ●; Rohr, Δ; scaled by 0.33; Jain and Thompson, – – –. For the 010 excitation: present data, O.

similar observation has been made by Sanche and Schulz (1973) for the corresponding shape resonance in H_2O. This H_2O^- resonance has been studied in vibrational excitation by Seng and Linder (1976). Using the formalism of Read (1968) for the qualitative analysis of resonance features, they obtained a best fit to their (100, 001) angular distribution using a superposition of s- and d-wave contributions, consistent with the $^2A_1$ symmetry.

On the other hand, the eigenphase analysis of both Jain and Thompson (1983) and Gianturco (1991) of the possible H_2S^- states in this region, indicated that this resonance was of $^2B_2$ symmetry. Further, recent calculations and symmetry analyses by Gallup (1993) show the $^2B_2$ state lies about 3 eV below the $^2A_1$, and that the former is predominantly d-wave in character, thus corroborating the earlier theoretical assignment. Close examination of the present results, at both 2.0 and 3.0 eV (figure 11), reveals angular distributions which are not isotropic but which show, for both modes, the clear presence of a d-wave contribution as well as a strong contribution from direct dipole scattering in the 100 + 001 mode. Such an angular distribution is apparently compatible with either of the above classifications and as such the present work cannot really be used to discriminate between them.

4. Conclusions

The present data represent the first comprehensive set of absolute elastic differential cross section measurements for low energy electron scattering from H_2S. They provide an ideal test for several recent theoretical models, in particular the complex Kohn variational approach (Lengsfield *et al* 1992), which has previously been shown to provide an adequate description of e^-–NH_3 elastic scattering. It appears that the level of agreement, both qualitative and quantitative, is somewhat better in the present case. At those energies where a comparison

is possible there is also good agreement with the calculation of Jain and Thompson (1983) and, at higher energies, there is good agreement with the calculation of Gianturco (1991). The agreement between the present results and the relative measurements of Marinkovic (1985) is remarkably good at all energies and scattering angles. The situation for vibrational excitation is not so clear with conflicting comparisons between the absolute magnitude of the present cross sections and those from both experiment and theory for the two vibrational bands studied.

Acknowledgments

We are grateful to Dr Byron Lengsfield for providing tabulated values of the Kohn variational cross sections prior to publication and to Dr Cz Szmytkowski for sending us tabulated values of the data of Dr Marinkovic. It is a pleasure to acknowledge discussions with Gordon Gallup concerning the nature of the low-lying shape resonance. The experimental measurements would not have been possible without the expert technical assistance and support from Graeme Cornish, John Gascoigne and Kevin Roberts. RJG thanks the Australian National University for the provision of a Postgraduate Research Award.

References

Alle D T, Gulley R J, Buckman S J and Brunger M J 1992 *J. Phys. B: At. Mol. Opt. Phys.* **25** 1533
Andrick D and Bitsch A 1975 *J. Phys. B: At. Mol. Phys.* **8** 393
Azria R, Le Coat Y, Lefevre G and Simon D 1979 *J. Phys. B: At. Mol. Phys.* **12** 679
Brunger M J, Buckman S J, Allen L J, McCarthy I E and Ratnavelu K 1992 *J. Phys. B: At. Mol. Opt. Phys.* **25** 1823
Brunger M J, Buckman S J and Newman D S 1990 *Aust. J. Phys.* **43** 665
Brunger M J, Buckman S J, Newman D S and Alle D T 1991 *J. Phys. B: At. Mol. Opt. Phys.* **24** 1435
Brunt J N H, King G C and Read F H 1977 *J. Phys. B: At. Mol. Phys.* **10** 1289
Buckman S J, Gulley R J, Bennett S J and Moghbelalhossein M 1993 *Meas. Sci. Technol.* in press
Fiquet-Fayard F, Ziesel J P, Azria R, Tronc M and Chiari J 1972 *J. Chem. Phys.* **56** 2540
Gallup G A 1993 Private communication
Gianturco F A 1991 *J. Phys. B: At. Mol. Opt. Phys.* **24** 4627
Gianturco F A and Thompson D G 1983 *J. Phys. B: At. Mol. Phys.* **13** 613
Gulley R J, Brunger M J and Buckman S J 1992 *J. Phys. B: At. Mol. Opt. Phys.* **25** 2433
Jain A and Thompson D G 1983 *J. Phys. B: At. Mol. Phys.* **17** 443
Lengsfield B H, Rescigno T N, McCurdy C W and Parker S 1992 Private communication
Marinkovic B P 1985 *PhD Thesis* University of Beograd (unpublished)
Nesbet R K 1979 *Phys. Rev.* A **20** 58
Nickel J C, Zetner P W, Shen G and Trajmar S 1989 *J. Phys. E: Sci. Instrum.* **22** 730
Norcross D W and Collins L A 1982 *Adv. At. Mol. Phys.* **18** 341
Read F H 1968 *J. Phys. B: At. Mol. Phys.* **1** 893
Rescigno T N, Orel A E, Hazi A U and McKoy B V 1982 *Phys. Rev.* A **26** 690
Rohr K 1978 *J. Phys. B: At. Mol Phys.* **11** 4109
Sanche L and Schulz G J 1973 *J. Chem. Phys.* **58** 479
Seng G and Linder F 1976 *J. Phys. B: At. Mol. Phys.* **9** 2539
Shi X and Burrow P D 1992 *J. Phys. B: At. Mol. Opt. Phys.* **25** 4273
Sokolov V F and Sokolova Yu A 1981 *Sov. Tech. Phys. Lett.* **7** 268
Szmytkowski Cz and Maciag K 1986 *Chem. Phys. Lett.* **129** 321